

Commutability between Semiclassical Limit and Adiabatic Limit

Biao Wu¹ and Jie Liu²

¹*Institute of Physics, Chinese Academy of Sciences, P.O. Box 603, Beijing 100080, China*

²*Institute of Applied Physics and Computational Mathematics, P.O. Box 8009, Beijing 100088, China*

(Dated: July 30th, 2005)

We study the adiabatic limit and the semiclassical limit with a second-quantized two-mode model, which describes a many-boson interacting system. When its mean-field interaction is small, these two limits are commutable. However, when the interaction is strong and over a critical value, the two limits become incommutable. This change of commutability is associated with a topological change in the structure of the energy bands. These results reveal that nonlinear mean-field theories, such as Gross-Pitaevskii equations for Bose-Einstein condensates, can be invalid in the adiabatic limit.

PACS numbers: 03.65.Sq, 05.45.Mt, 03.75.Lm

The experimental creation of Bose-Einstein condensates (BECs) with dilute alkali atomic gases has generated great excitement and literally created a new subfield in physics[1, 2]. One of the main reasons is that it has made it possible to test experimentally some fundamental and important physics that could only be discussed theoretically before. For instance, Tonks-Girardeau gas and quantum phase transition between superfluid and Mott insulator has been studied by theorists since 1960s; they were observed experimentally only recently with BECs[3, 4]. There are now even discussions on how to use BECs to study black holes[5] and superstrings[6].

In this Letter we discuss a fundamental concept in quantum mechanics, the commutability of the semiclassical limit and the adiabatic limit, with a second-quantized two-mode model. We suggest a possible experimental testing of this concept with BECs. This concept is due to M.V. Berry[7]. In brief, consider a quantum system whose Hamiltonian is time-dependent,

$$i\hbar \frac{\partial}{\partial t} |\psi\rangle = H(\mathbf{R}(\alpha t)) |\psi\rangle. \quad (1)$$

One can eliminate α from the above Schrödinger equation with a scaled time $\tau = \alpha t$ and an effective Plank constant $\tilde{\hbar} = \alpha \hbar$. With this scaling argument, Hwang and Pechukas claimed that the semiclassical limit $\tilde{\hbar} \rightarrow 0$ and the adiabatic limit $\alpha \rightarrow 0$ are equivalent[8].

This point was refuted by Berry[7], who pointed out that these two limits are not equivalent because the Hamiltonian H may depend implicitly on $\tilde{\hbar}$. Moreover, he showed that these two limits are incommutable in a simple double-well model: the Landau-Zener (LZ) tunneling rate in this model is zero if the adiabatic limit $\alpha \rightarrow 0$ is taken first; it becomes one when the semiclassical limit $\tilde{\hbar} \rightarrow 0$ is taken first[7]. Since it is impossible to change $\tilde{\hbar}$ experimentally, this concept has remained a game of theorists.

We revisit the commutability between the semiclassical limit and the adiabatic limit with a second-quantized two-mode tunneling model. This model can be used to

describe a BEC system where only two quantum states are important, such as in a double-well potential or with two internal quantum states[2, 9]. In this model, the semiclassical limit is $N \rightarrow \infty$ with N being the number of bosons. In this large N limit, the second-quantized model becomes a two-level mean-field model. We show that one can recover the second-quantized model by quantizing this mean-field model with the Sommerfeld rule. As N can be changed in experiments, the semiclassical limit becomes experimentally accessible.

More interestingly, the commutability between the two limits, $N \rightarrow \infty$ and $\alpha \rightarrow 0$, in this second-quantized model depends on its mean-field interaction strength c . If c is small, the two limits are commutable; when c is over a critical value, the two limits become incommutable. Such a dependence on c is found to be related to a topological change in the structure of the energy bands. These results indicate that nonlinear mean-field theories, such as Gross-Pitaevskii equations for BECs, can be invalid in the adiabatic limit when the mean-field interaction is strong. Finally, we discuss how this commutability can be tested in a BEC experiment.

The second-quantized two-mode model is

$$\hat{H} = \frac{\gamma}{2}(\hat{a}^\dagger \hat{a} - \hat{b}^\dagger \hat{b}) + \frac{v}{2}(\hat{a}^\dagger \hat{b} + \hat{a} \hat{b}^\dagger) - \frac{\lambda}{4}(\hat{a}^\dagger \hat{a} - \hat{b}^\dagger \hat{b})^2, \quad (2)$$

where generators and annihilators \hat{a}^\dagger, \hat{a} and \hat{b}^\dagger, \hat{b} are for two different quantum states. In the Hamiltonian \hat{H} , γ is the energy offset between the two quantum states and changes with time as $\gamma = \alpha t$. The parameter v measures the coupling between the two states while $\lambda > 0$ is the interacting strength between bosons. The minus sign before λ indicates that the interaction is attractive. In this system the total number of bosons N is conserved.

For this second-quantized model, its semiclassical limit is $N \rightarrow \infty$. In such a limit, the system's dynamics is given by the following nonlinear two-level model,

$$i \frac{d}{dt} \begin{pmatrix} a \\ b \end{pmatrix} = \left\{ \left[\frac{\gamma}{2} - \frac{c}{2}(|a|^2 - |b|^2) \right] \sigma_z + \frac{v}{2} \sigma_x \right\} \begin{pmatrix} a \\ b \end{pmatrix}. \quad (3)$$

where $c = N\lambda$ and $|a|^2 + |b|^2 = 1$. This model is often called a mean-field model. Technically to obtain the mean-field model, one focuses on the Gross-Pitaevskii states[2] $|\Psi_{gp}\rangle = \frac{1}{\sqrt{N!}}(a\hat{a}^\dagger + b\hat{b}^\dagger)^N|\text{vac}\rangle$. By computing the expectation value $\langle\hat{H}\rangle = \langle\Psi_{gp}|\hat{H}|\Psi_{gp}\rangle$, one obtains the mean-field Hamiltonian $H_{\text{mf}} = \langle\hat{H}\rangle/N$ (up to a trivial constant) in the limit of $N \rightarrow \infty$. The Hamiltonian H_{mf} leads to the dynamics in Eq.(3). For a rigorous account of large N limit as a semiclassical limit in models such as Eq.(2), we refer readers to Ref.[11].

We emphasize that the semiclassical limit $N \rightarrow \infty$ is taken with the mean-field interaction strength $c = N\lambda$ kept constant. Physically, this is to ensure that the series of systems with different N 's have about the same physics. If λ were kept constant instead of c , the last term in Eq.(2) would become too dominating at the large N limit, completely changing the physics of the system. When the model (2) is used to describe a BEC in a double-well potential, the limit $N \rightarrow \infty$ at a constant c is equivalent to having a larger trap for more atoms in the BEC, or to tuning λ smaller with the Feshbach resonance technique[12].

We are interested in how the second-quantized model Eq.(2) behaves in the two limits, $N \rightarrow \infty$ and $\alpha \rightarrow 0$, in particular, whether the model's behavior depends on which limit is taken first. For this purpose, we follow Berry's methodology[7] to focus on the tunneling behavior of the quantized model.

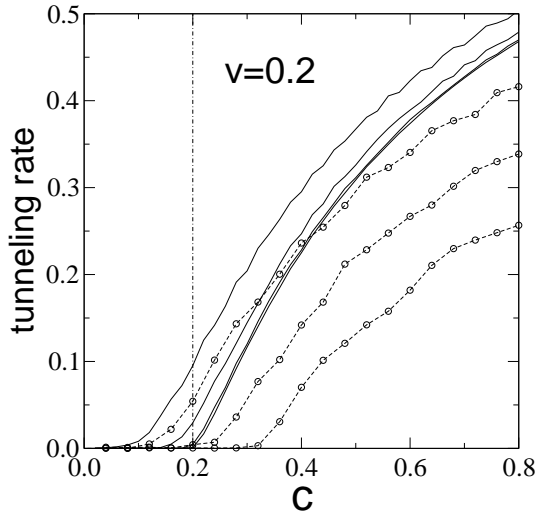


FIG. 1: Tunneling rate as a function of the mean-field interaction strength c . The solid lines are obtained with the mean-field model (3) for $\alpha = 0.005, 0.001, 0.0001, 0.00001$ (from top to bottom); the circle-dashed lines are with the quantized model (2) for $\alpha = 0.005, 0.001, 0.0001$ (from top to bottom). $N = 8$ and $v = 0.2$ are used.

In Fig.1 the tunneling rates are plotted as a function of the mean-field interaction strength c . Two sets of tunneling rates are calculated: one with the quantized

model (2) for a fixed number of bosons; the other with the mean-field model (3). In computing the tunneling rate, we have assumed that the system is completely in state a at $t \rightarrow -\infty$; the tunneling rate is the probability of remaining in state a at $t \rightarrow \infty$, the end of dynamical evolutions. At a fixed number of bosons, the dynamics of the quantized model (2) can be found by expanding a quantum state in terms of Fock states $|N_a, N_b\rangle$, where N_a and N_b are numbers of particles in quantum states a and b , respectively. In terms of $|N_a, N_b\rangle$, the Hamiltonian becomes a $(N+1) \times (N+1)$ matrix.

Upon careful examination of the data in Fig.1, one notices that $c = v$ is a critical value. When $c < v$, the tunneling rate goes to zero in the adiabatic limit $\alpha \rightarrow 0$ for both the mean-field model and the quantized model. However, when $c > v$, the tunneling rate from the mean-field model is always non-zero while the tunneling rate can be zero for the quantized model. Since the mean-field model is the semiclassical limit of the quantized model, the mean-field result can be regarded as the result from the quantized model with the limit $N \rightarrow \infty$ having been taken. Therefore, the results in Fig.1 show that the tunneling behavior in the quantized model (2) depends strongly on the order of the limits taken while this dependence itself relies on the value of the mean-field interaction strength c .

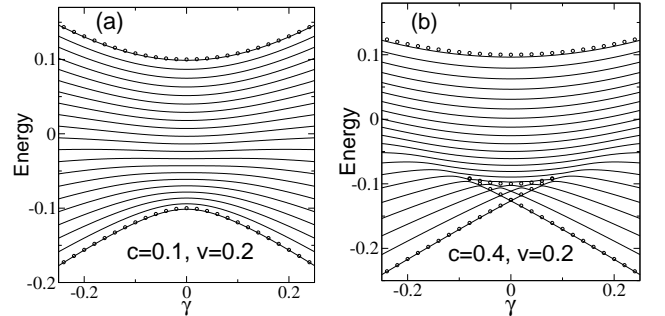


FIG. 2: Energy levels from the second-quantized model \hat{H} ($N = 20$) and the mean-field model H_{mf} . The solid lines are quantized energy levels; the open circles are mean-field energy levels. Note that for comparison with the mean-field theory, the quantized energy levels from \hat{H} have been divided by N .

To understand the above results, we first examine the energy levels of the second-quantized model (2) as functions of γ , the slowly changing system parameter. These energy levels can be found by directly diagonalizing the Hamiltonian \hat{H} and they are plotted in Fig.2. There is a drastic change in the structure of energy levels as the mean-field interaction c changes: a net of anti-crossings appears in the lower part of the quantized energy levels when $c > v$. As known before[14], when $c > v$ there is a loop structure emerging in the energy band of the mean-field model (3). When the mean-field energy levels (circles) are also plotted in Fig.2, we find that the quantized energy levels are bounded by the mean-field energies. In

particular, the mean-field energy levels envelop the net of anti-crossings in the quantized energy levels. Such a correspondence was first noticed in Ref.[9].

The structure change in the energy bands is associated with a change in the phase space of the mean-field model (3) as shown in Fig.3. In plotting this figure, we notice that the mean-field model, in fact, has only two independent variables and its Hamiltonian can be reduced to

$$H_{\text{mf}} = \gamma p + \frac{v}{2} \sqrt{1 - 4p^2} \cos q - cp^2, \quad (4)$$

where $p = (|a|^2 - |b|^2)/2$ and $q = \theta_b - \theta_a$ with $\theta_{a,b}$ being the phases of a and b . It is clear from Fig.3, when $c < v$, there is one minimum and one maximum; when $c > v$, we see two local minima, one maximum and one saddle point. Since these extremum points correspond to the eigenstates in the mean-field energy bands in Fig.2[10], the structure change in the phase space is apparently connected with the structure change in the energy levels.

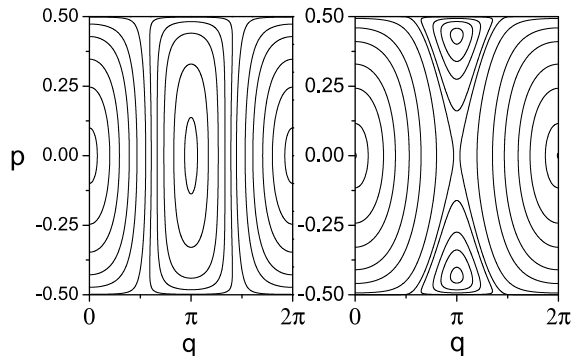


FIG. 3: Energy contours of the mean-field model H_{mf} . Left: $c = 0.1$, $v = 0.2$, $\gamma = 0.0$; right: $c = 0.4$, $v = 0.2$, $\gamma = 0.0$.

This connection can be further explored by re-quantizing the mean-field model H_{mf} with the Sommerfeld theory, which says that the quantum motions are the periodic motions in the classical phase space that satisfy

$$\frac{1}{2\pi} \oint p dq = n\hbar/N, \quad n = 0, 1, 2, \dots \quad (5)$$

The division by N comes from the fact that the mean-field Hamiltonian is an average for one particle, $H_{\text{mf}} = \langle \hat{H} \rangle / N$. One can view $\hbar_{\text{eff}} = \hbar/N$ as the effective Plank constant for H_{mf} . In our calculations, the natural unit $\hbar = 1$ is used. For convenience, we shall call the energy levels obtained with Eq.(5) the Sommerfeld energy levels. They are shown and compared to the quantized energy levels of \hat{H} in Fig.4.

When $c < v$, the mean-field Hamiltonian has exactly one maximum ($q = 0$) and one minimum ($q = \pi$). The Sommerfeld quantization around the maximum produces energy levels lower than the maximum energy while the

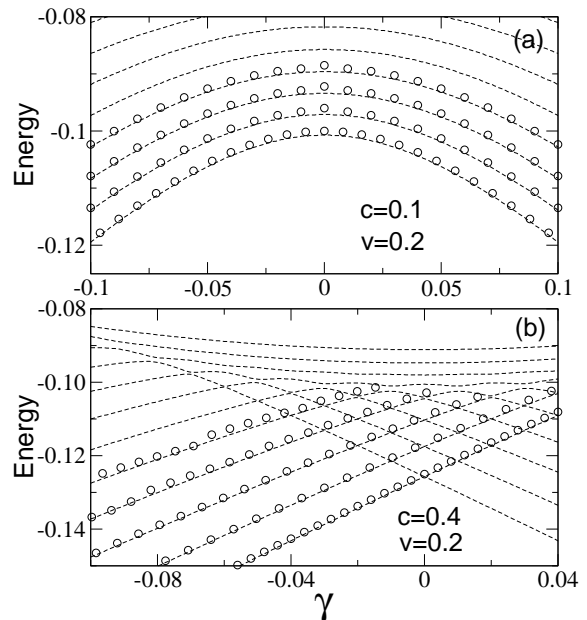


FIG. 4: Comparison between the energy levels of the second-quantized model (dashed line) with $N = 40$ and the Sommerfeld energy levels (open circles). (a) $c = 0.1$, $v = 0.2$; (b) $c = 0.4$, $v = 0.2$. For clarity, we have plotted only a portion of the energy levels.

quantization around the minimum generates energy levels higher than the minimum. This explains why the mean-field energy levels bound the quantized energy levels in Fig.2. We also see that the energy gap arises from the different quantization number in Eq.(5), from which we estimate that the energy gap between the lowest two energy levels at $\gamma = 0$ is $\Delta \approx v\sqrt{1 - c/v}$, independent of N . This agrees well with the numerical results in Fig.5.

When $c > v$, the phase space of H_{mf} becomes very different: there are two local minima with an additional saddle point. In this case, the Sommerfeld quantization around the two local minima gives rise to two sets of Sommerfeld energy levels. In the lower part of Fig. (4), for clarity, we have plotted only one set. If two sets were plotted, they would form a net of crossings, matching very well with the anti-crossing net from \hat{H} . In doing the Sommerfeld quantization, we have ignored the tunneling through the energy barrier between the two local minima. Once the tunneling is considered, degeneracies are lifted and the crossings become anti-crossings. This shows the energy gaps inside the triangular net have a different origin from the energy gaps outside the net or in the case of $c < v$. The energy gaps produced at these crossings can be estimated with the WKB method. Since the effective Planck constant for H_{mf} is \hbar/N , we expect that the gaps decrease exponentially with N . This is exactly what the numerical results in Fig.5 indicates.

It is now not difficult to understand the tunneling behavior that we have seen in Fig.1. Let us recall the

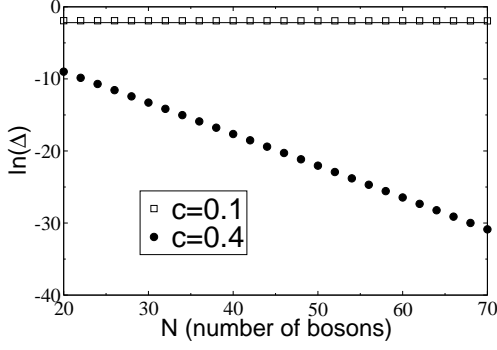


FIG. 5: Energy gap between the lowest two eigen-energies in the second-quantized model at $\gamma = 0$. The squares are for $c = 0.1$ and the dots for $c = 0.4$, with $v = 0.2$ for both. The solid line is an approximation result $\Delta = v\sqrt{1 - c^2/v^2}$ for $c < v$.

Landau-Zener tunneling in a two-level model[13]. As γ changes with time as $\gamma = \alpha t$, the LZ tunneling rate is $r_{\text{LZ}} = \exp\left(-\frac{\pi\Delta^2}{2\alpha}\right)$, where Δ is the energy gap between the two levels. For a multi-level system like our second-quantized model \hat{H} , the above equation should still be a very good approximation for the tunneling rate between two consecutive energy levels. We use the tunneling between the two lowest energy levels as an example. As already analyzed, the energy gap changes with N as follows,

$$\Delta = \begin{cases} \kappa_1 v & c < v, \\ N\kappa_2 \exp(-\eta N) & c > v. \end{cases} \quad (6)$$

The parameter $\kappa_1 \approx \sqrt{1 - c/v}$. The other two parameters κ_2 and η can be computed with the WKB method as in Ref.[7] or with a more sophisticated method[15]. This leads to the following tunneling rate

$$r \sim r_{\text{LZ}} = \begin{cases} \exp\left(-\frac{\pi\kappa_1^2 v^2}{2\alpha}\right) & c < v, \\ \exp\left(-\frac{\pi N^2 \kappa_2^2}{2\alpha e^{2\eta N}}\right) & c > v. \end{cases} \quad (7)$$

For the case of $c < v$, it is clear that we have

$$\lim_{N \rightarrow \infty} \lim_{\alpha \rightarrow 0} r = \lim_{\alpha \rightarrow 0} \lim_{N \rightarrow \infty} r = 0, \quad (8)$$

which shows that the two limits $\alpha \rightarrow 0$ and $N \rightarrow \infty$ are commutable. This explains why when $c < v$, both sets of the tunneling rates in Fig.1 become zero as $\alpha \rightarrow 0$.

For the other case $c > v$, the tunneling rate takes different values at two different limits:

$$\begin{cases} \lim_{N \rightarrow \infty} \lim_{\alpha \rightarrow 0} r = 0, \\ \lim_{\alpha \rightarrow 0} \lim_{N \rightarrow \infty} r > 0. \end{cases} \quad (9)$$

This reveals that the two limits are no longer commutable. In the first limit, the adiabatic limit $\alpha \rightarrow 0$

is taken at a fixed number of bosons, for which the energy gap is finite and one can always be slow enough not to causing tunneling. In the second limit, since the energy gap is already closed at $N \rightarrow \infty$, tunneling occurs no matter how slow γ changes. This explains why the tunneling rate from the mean-field model is always non-zero for $c > v$. This incommutability of these two limits also implies that the mean-field theories, such as Gross-Pitaevskii equation for BECs, can be invalid for the adiabatic limit. One example is the Bloch states for a BEC in an optical lattice is studied. In such a system, the Bloch wavenumber k can be regarded as an adiabatic parameter. If the Gross-Pitaevskii equation were always valid in the adiabatic limit, it would mean that stable Bloch states should exist for all possible k . However, as shown in Ref.[16], a significant portion of Bloch states are unstable.

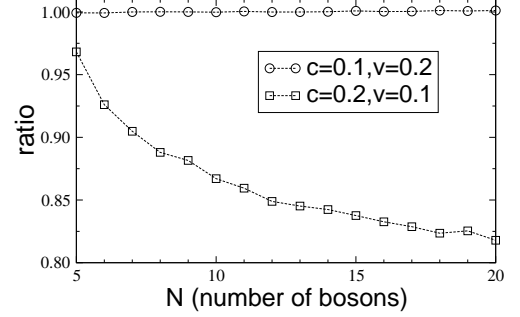


FIG. 6: Ratio of the bosons in the right well at the end of tunneling process. The computation is done with the second-quantized model \hat{H} with a sweeping rate $\alpha = 0.0001$.

With cold atomic gases, we believe that it is now possible to test experimentally the commutability between the semiclassical limit and the adiabatic limit. For instance, one can load a BEC into a double-well potential generated by two laser beams[17]. The energy offset γ can be created by using different intensity for the two laser beams. To keep the mean-field interaction parameter c constant for different boson numbers, one can either use the Feshbach resonance technique[12] to adjust the interaction between atoms or change the size of the trap. In experiments, it is hard to measure the tunneling rate r between the two lowest energy levels as we just discussed. However, one can easily measure the number of atoms in either of the two potential wells. Once the experiment is set up, the most striking observation will be as shown in Fig.6. For $c < v$, if the system initially has all its atoms in the left well (quantum state a), then all the atoms will be in the right well for a fixed but very small sweep rate. It does not depend on N . For $c > v$, not all the atoms will fall into the right well: larger N less atoms in the right well. This difference illustrate our theoretical results on the commutability of the two limits, $\alpha \rightarrow 0$ and $N \rightarrow \infty$.

J.L. is supported by NNSF of China (10474008).
 B.W. is supported by the “BaiRen” program of the
 Chinese Academy of Sciences and the 973 project
 (2005CB724508).

-
- [1] F. Dalfovo, S. Giorgini, L.P. Pitaevskii, and S. Stringari, *Rev. Mod. Phys.* **71**, 463 (1999).
 - [2] A.J. Leggett, *Rev. Mod. Phys.* **73**, 307 (2001).
 - [3] M. Greiner, O. Mandel, T. Esslinger, T.W. Hansch, and I. Bloch, *Nature* **415**, 39 (2002).
 - [4] B. Paredes *et al.*, *Nature* **429**, 277 (2004).
 - [5] P.O. Fedichev and U.R. Fischer, *Phys. Rev. Lett.* **91**, 240407 (2003); L.J. Garay, J.R. Anglin, J.I. Cirac, and P. Zoller, *Phys. Rev. Lett.* **85**, 4643 (2000).
 - [6] M. Snoek, M. Haque, S. Vandoren, and H.T.C. Stoof *cond-mat/0505055*.
 - [7] M.V. Berry, *J. Phys. A* **17**, 1225 (1984).
 - [8] J.T. Hwang and P. Pechukas, *J. Chem. Phys.* **67** 4640 (1977).
 - [9] Z.P. Karkuszewski, K. Sacha, and A. Smerzi, *Eur. Phys. J. D* **21**, 251 (2002).
 - [10] Jie Liu *et al.*, *Phys. Rev. A* **66**, 023404 (2002).
 - [11] L.G. Yaffe, *Rev. Mod. Phys.* **54**, 407 (1982); Wei-Min Zhang, Da Hsuan Feng, and R. Gilmore, *Rev. Mod. Phys.* **62**, 867 (1990).
 - [12] S. Inouye *et al.*, *Nature* **392**, 151 (1998); Ph. Courteille *et al.*, *Phys. Rev. Lett.* **81**, 69 (1998).
 - [13] C. Zener, *Proc. R. Soc. London A* **137**, 696(1932).
 - [14] Biao Wu and Qian Niu, *Phys. Rev. A* **61**, 023402 (2000); Jie Liu *et al.*, *Phys. Rev. A* **66**, 023404 (2002).
 - [15] A. Garg, *Phys. Rev. B* **64**, 094413 (2001); *Phys. Rev. B* **64**, 094414 (2001).
 - [16] Biao Wu and Qian Niu, *Phys. Rev. A* **64**, 061603 (2001).
 - [17] Y. Shin *et al.*, *Phys. Rev. Lett.* **92**, 050405 (2004).